Photoproduction of jets, prompt photons, and photon structure

Bernard Andrieu

LPNHE, Ecole polytechnique, IN2P3-CNRS, F-91128 Palaiseau, France

E-mail: `andrieu@in2p3.fr`

On behalf of the H1 and ZEUS collaborations.

Abstract. Recent results on the photoproduction of jets and prompt photons at HERA are reviewed. The measurements allow tests of the consistency of the QCD description of photon-proton interactions. QCD-inspired models of higher-order and non-perturbative processes, as implemented in Monte-Carlo programs, are confronted with results on jet substructure and event topology. Cross-section measurements are compared to perturbative QCD calculations at Next to Leading Order (NLO) using available photon parton density functions (pdfs), to give insight into the hadronic structure of the photon. The effective transverse momentum of partons in the proton is studied using prompt photons.

1. Introduction

At the positron-proton collider HERA, where 27.5 GeV positrons collide with 820 or 920 GeV protons, the dominant hard-scattering processes are hard photoproduction events: a quasi-real photon ($Q^2 \simeq 0$, where Q^2 is the virtuality of the photon) emitted by the positron collides with a parton in the proton, interacting either as a bare particle in direct interactions (Fig. 1(a)), or via a hadronic state fluctuation in resolved interactions (Fig. 1(b)). At the lowest order in the perturbative series expansion in α_s, two partons, or one parton and a photon, are emitted back-to-back in the transverse plane with equal transverse energies (E_T). Due to the QCD radiation and fragmentation

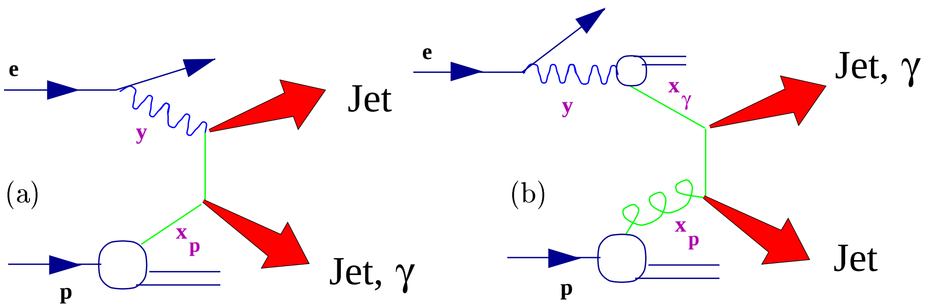

Figure 1. Examples of diagrams of jet-jet or jet-γ photoproduction in direct (a) and resolved (b) processes.

processes, the partons appear as collimated jets of particles, accompanied in general by the proton remnant and, in the case of resolved processes, by the photon remnant and by the particles resulting from a possible remnant-remnant interaction, also called the underlying event. The LO cross-section [1] can be expressed generically as:

$$\sigma^{ep\to e\,\mathrm{jet}\,\mathrm{jet}(\gamma)\,X}_{LO,\ \mathrm{dir.[res.]}} = \int d\Omega\ f_{\gamma/e}(y) \sum_{[i]j} [f_{i/\gamma}(x_\gamma, \mu_\gamma^2)]\ f_{j/p}(x_p, \mu_p^2) d\sigma(\gamma[i]\,j \to \mathrm{jet}\,\mathrm{jet}(\gamma)),$$

where $f_{\gamma/e}(y)$ is the photon flux in the positron in the equivalent photon approximation; $f_{i/\gamma}(x_\gamma, \mu_\gamma^2)$ ($f_{j/p}(x_p, \mu_p^2)$) is the pdf of parton i (j) inside the photon (proton); $d\sigma(\gamma[i]j \to \mathrm{jet}\,\mathrm{jet}(\gamma))$ is the cross-section for the direct subprocess $\gamma j \to \mathrm{jet}\,\mathrm{jet}(\gamma)$ or for the resolved subprocess $ij \to \mathrm{jet}\,\mathrm{jet}(\gamma)$, which is proportional to $(\alpha_{em}^n(\mu_R^2)\alpha_s^{2-n}(\mu_R^2))$ with $n = 0$, 1, or 2; μ_R is the renormalization scale; x_γ (x_p) is the fraction of the momentum of the photon (proton) taken by parton i (j); μ_γ (μ_p) is the QCD factorization scale in the photon (proton); and the sum runs over all partons j in the proton and, in the case of resolved processes, over all partons i in the photon. The proton pdfs are well known from F_2 measurements [2] down to very low x. For the photon, the quark density is constrained at medium and low x_γ from F_2^γ measurements [3] at e^+e^- colliders, but there is less information on the gluon density, boson-gluon fusion being a second order process compared to photon-quark scattering. In ep collisions, diagrams for direct processes are of order $\alpha_{em}\alpha_s$ (resp. α_{em}^2) for parton-parton (resp. parton-photon) production, compared to α_s^2 (resp. $\alpha_{em}\alpha_s$) for resolved processes. However, since the photon pdfs are proportional to α_{em}/α_s in the asymptotic limit of large μ_γ, the direct and resolved contributions are of comparable size, the resolved being less prominent as the E_T of the outgoing partons increases. The clear separation between the direct and the resolved diagrams is, of course, only valid at LO and depends on the choice of a cut-off scale on the $\gamma \to q\bar{q}$ branching.

Studying high E_T jets and prompt photons presents several advantages. The value of E_T of the outgoing partons gives a natural hard scale which allows cross-section calculations in perturbative QCD to be made. For jets, the high E_T of the corresponding parton going out of the hard process also ensures a reduced influence of less-well understood soft processes, such as hadronization and the soft underlying event. The uncertainty due to hadronization is smaller for prompt photons. Jets and prompt photons at high E_T thus provide the most direct insight into photoproduction at the parton level.

From the experimental point of view, results are obtained from individual particles with their momentum (tracks from charged particles) or energy (clusters from all particles, except muons and neutrinos) measured in detectors. At the same time, the most accurate QCD calculations, presently available at NLO, are expressed only at the parton level. A gap has to be bridged in either direction in order to make meaningful comparisons: the influence of the (imperfect) detector has to be taken out in order to get the measured experimental cross-sections back to the hadron level, while the effect of hadronization must be taken into account on the theoretical cross-sections.

We will first present results on jet substructure, which prove the correctness of the phenomenological Monte-Carlo models of higher order (QCD radiation) and soft (fragmentation) processes, as well as of the remnant and underlying event, and give confidence in the extraction of cross-sections at the hadron level by using the same Monte-Carlo simulations. By allowing a separation between quark and gluon jets, these measurements also provide tests of the spin structure of parton-parton dynamics.

Measurements of various jet (inclusive, dijet, 3-jet) cross-sections will then be presented. The most accurate theoretical calculations using available photon pdfs, at NLO for the two first, and at LO for the last one, are confronted with data. Since the presence of a peak in any E_T or invariant mass spectrum would be a sign for unexpected physics, they allow for searches of physics beyond the Standard Model. Dijet events, where a full kinematic reconstruction of x_γ is possible, give access to the photon pdfs at previously unreached scales, in particular to the gluon component of the photon. Measurements of various angular distributions in dijet and 3-jet events also allow the study of the polarization of the exchanged particle in the partonic subprocess.

Finally, prompt photon measurements will be shown, which can again be compared to NLO QCD calculations. In addition, the photon can act as a test particle to probe the intrinsic transverse momentum of partons in the proton.

Since most of the results reviewed here use similar experimental procedures, we will not repeat the technical details for each analysis. Unless otherwise stated, the results presented below share the following experimental features:

- events were required to have a photon energy fraction (y) in the interval $0.2 < y < 0.9$ and a photon virtuality $Q^2 \leq 1$ GeV^2;
- jets were found using the inclusive k_T algorithm [4], which successively combines neighboring particles. It is factorizable, and it is infrared-safe to all orders;
- jets were required to have a transverse energy $E_T^{jet} > 14$ GeV and to be contained in the pseudorapidity (η) interval $-1 < \eta^{jet} < 2.5$;
- data were corrected for detector effects to give results at the hadron level. For experimental studies of detector corrections, two Monte-Carlo programs were used: PYTHIA [5] and HERWIG [6]. Both are based on LO QCD cross-section calculations, and include initial and final state QCD radiation corrections to simulate higher-order processes. They differ in the treatment of fragmentation and of the underlying event. PYTHIA uses the Lund string model [7] for fragmentation, and simulates the underlying event in the Multiple Interaction (MI) scheme as the result of additional interactions between partons from the photon and proton remnants. HERWIG uses a cluster fragmentation scheme [8], and simulates the underlying event by adding minimum bias events to an adjustable fraction of the resolved processes. This fraction is generally fixed to a value around 35%.

For presentation of data and comparison with theory, the following common features will be used:

- the inner error bars will show the statistical errors, and the outer the statistical and uncorrelated systematic errors added in quadrature. The correlated systematic error is essentially due to the largest systematic error, associated with the hadronic energy scale uncertainty of $\pm 4\%$, which gives an uncertainty of 15 to 20% on cross-sections and is shown separately as a shaded band;
- for NLO QCD calculations, several programs are available from different groups: Frixione *et al.* [9], Klasen and Kramer [10], Harris and Owens [11], Aurenche *et al.* [12]. Since all these programs agree within 5 to 10 %, the result of only one of these calculations will be given for each experimental result;
- in NLO calculations, the pdfs used will be CTEQ4M or CTEQ5M [13] for the proton, and GRV [14], AFG [15] or GS [16] for the photon.

2. Jet substructure

ZEUS has presented preliminary results [17] on the detailed characteristics of jets in photoproduction. Two variables were used for these studies, the mean jet shape $<\psi(r)>$ and the mean subjet multiplicity $<n_{\rm subjet}(y_{cut})>$. A distance Δ_{ij} between two "particles" i and j, i.e. two reconstructed objects from the detector, is first defined as: $\Delta_{ij} = \sqrt{(\eta_i - \eta_j)^2 + (\varphi_i - \varphi_j)^2}$. Using this distance, the jet shape $\psi(r)$ is defined as the fraction of transverse energy in a cone of radius $R = 1$ around the jet axis which is contained in a cone of a smaller radius r. By definition, $\psi(r = R) = 1$. Once jets have been found using the inclusive k_T algorithm, subjets inside jets can be resolved by again applying the k_T algorithm for a given value of $y_{\rm cut}$, until for every pair of "particles" i

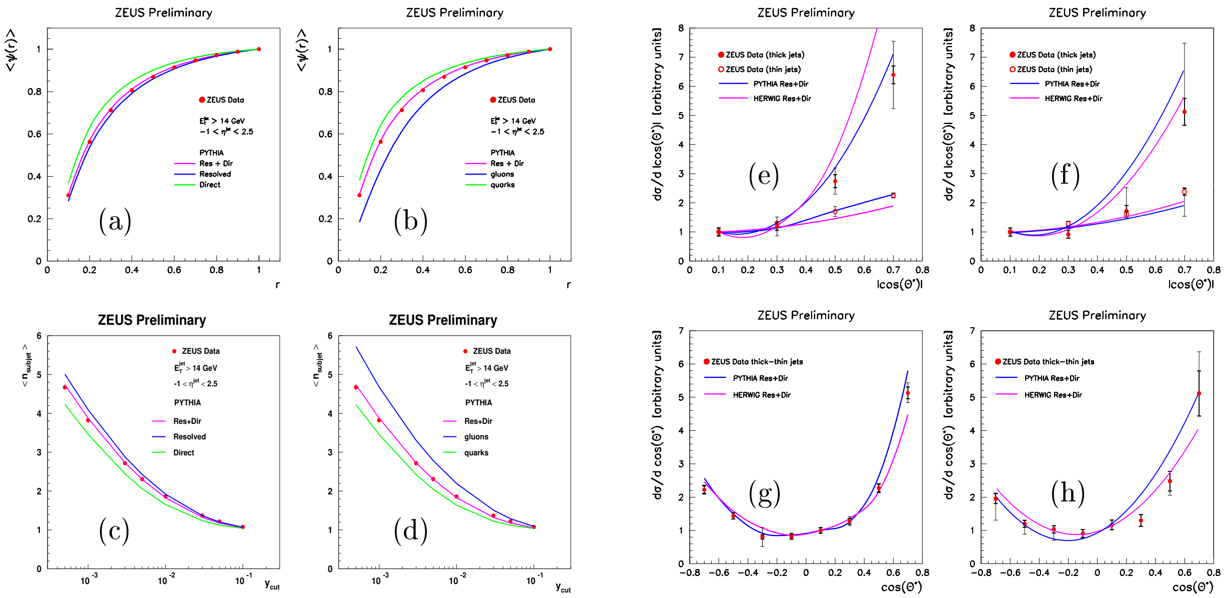

Figure 2. Left: jet shape (a,b) and subjet multiplicity (c,d), compared to PYTHIA prediction, separated in resolved and direct (a,c) and gluons and quarks (b,d). Right: $\cos\theta^*$ distribution for events with 2 "gluon" vs 2 "quark" jets (e,f), and with 1 "gluon" and 1 "quark" jet (g,h), where jets are classified as "gluon" or "quark" according to their shape (e,g) or subjet multiplicity (f,h).

and j: $d_{ij} = \min(E_{Ti}, E_{Tj})^2 \Delta_{ij}^2 \geq y_{\rm cut}(E_T^{jet})^2$, then counting the corresponding number of remaining subjets $n_{\rm subjet}$. By definition, $n_{\rm subjet} = 1$ for $y_{\rm cut} \geq 1/4$. The measured $<\psi(r)>$ and $<n_{subjet}(y_{cut})>$ are shown in Fig. 2(a,b) and Fig. 2(c,d), and are compared to the PYTHIA prediction, separated into resolved and direct contributions (Fig. 2(a,c)) and into quark and gluon contributions (Fig. 2(b,d)). PYTHIA gives a very good description of the data, and predicts that gluon-initiated jets are broader and contain more subjets than quark jets. A statistical separation is then possible between "quark" (= thin) and "gluons" (= thick) jets, which can be tested by measuring the angular distribution of jets for samples separated according to either of these two variables.

The measurement of the angle θ^* of the two outgoing partons with respect to the beam axis in the parton-parton centre-of-mass system allows tests of the spin structure of the underlying parton dynamics. This angle can be reconstructed from $\cos\theta^* = \left|tanh\frac{(\eta_1-\eta_2)}{2}\right|$, using the two most energetic jets of the event. Its distribution is sensitive to the convolution product of matrix elements with phase space. For resolved interactions, dominated by gluon exchange, the spin 1 of the exchanged particle implies $d\sigma/dcos\theta^* \sim (1-|cos\theta^*|)^{-2}$ as $|cos\theta^*| \rightarrow 1$, while for direct interactions, dominated by quark exchange, the spin 1/2 of the exchanged particle implies $d\sigma/dcos\theta^* \sim (1-|cos\theta^*|)^{-1}$ when $|cos\theta^*| \rightarrow 1$. The preliminary ZEUS measurements, based on dijet events with $M^{JJ} > 47$ GeV, are shown for events involving various combinations of "quark" and "gluon" jets, where jets are separated according to their shape (Fig. 2(e,g)) or subjet multiplicity (Fig. 2(f,h)). The measured $d\sigma/d|\cos\theta^*|$ is shown in Fig. 2(e,f) for events with either 2 "gluon" or 2 "quark" jets. Since the two jets cannot be distinguished, only the absolute value $|\cos\theta^*|$ can be reconstructed. The expected different behaviour of the angular distribution for the two samples is well reproduced by Monte-Carlo simulation. For events with one "gluon" and one "quark" jet, the sign can be determined, and $d\sigma/d\cos\theta^*$ is presented in Fig. 2(g,h). Its asymmetric behaviour, reasonably described by PYTHIA and HERWIG, can be understood in terms of the dominant resolved subprocess $q_\gamma g_p \rightarrow qg$, which involves two diagrams: t-channel gluon exchange dominates as $\cos\theta^* \rightarrow 1$, while u-channel quark exchange dominates as $\cos\theta^* \rightarrow -1$. These results confirm that the method of separation between "quark" and "gluon" jets is meaningful, and that the spin structure and the dynamics of the partonic interaction are well understood.

3. Inclusive jet production

Inclusive jet cross-sections have been measured by both ZEUS [18] and H1 [19] in similar conditions. ZEUS kept events with $Q^2 \leq 4$ GeV^2 but restricted the acceptance of jets to $-0.75 < \eta^{jet} < 2.5$, while H1 measured cross-sections in a slightly extended y range of $0.1 < y < 0.9$, but only for jets with $E_T^{jet} > 21$ GeV.

The cross-section $d\sigma/dE_T^{jet}$ is presented for ZEUS (Fig. 3(a,b)) and H1 (Fig. 3(c,d)). The measured cross-sections compared to various predictions are shown in Fig. 3(a,c), and the relative differences between the measurements and the NLO predictions with

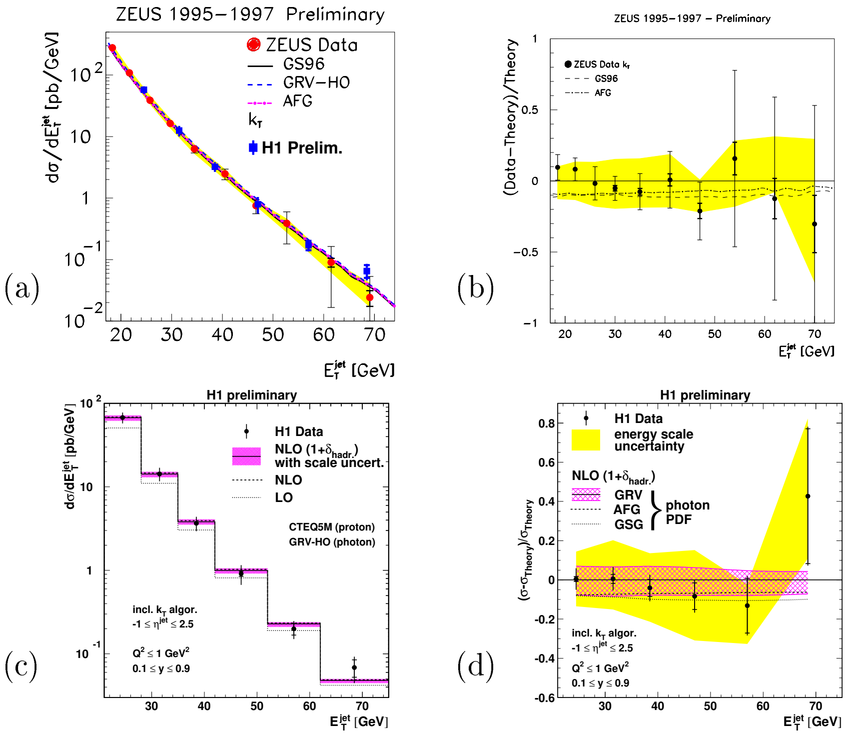

Figure 3. Inclusive $d\sigma/dE_T^{jet}$ measurements (a,c) and relative differences between measurements and calculations (b,d), for ZEUS (a,b) and H1 (c,d).

different photon pdfs in Fig. 3(b,d). The ZEUS result (Fig. 3(a)) is found in agreement with an H1 measurement obtained using exactly the same cuts as in the ZEUS analysis. The cross-section measured by H1 is also compared to QCD calculations at LO and NLO including hadronization corrections, denoted as NLO(1+δ_{had}). The LO calculation is clearly unable to reproduce the data at low E_T^{jet}. The hadronization corrections of the NLO prediction for H1 are small. The uncertainty of NLO(1+δ_{had}), when varying the factorization and renormalization scales by a factor 2 up and down, is shown as a hatched band. All NLO predictions are in good agreement with ZEUS and H1 results, but the sizes of both experimental and theoretical errors do not allow one to discriminate between the different photon pdfs.

4. Dijet production and photon structure

Two new measurements of dijets at high E_T^{jet} have been presented by ZEUS [20] and H1 [21]. Events were selected according to the E_T of the two hardest jets, by imposing the conditions: $E_T^{jet1} > E_1$ and $E_T^{jet2} > E_2$, with E_1 (E_2) = 14 (11) GeV in ZEUS, and E_1 (E_2) = 25 (15) GeV in H1. The presence of two jets allows the reconstruction of the fraction x_γ of the photon energy taken by a parton, using the LO formula: $x_\gamma^{jets} = (\sum_{jet}(E - p_z))/2E_\gamma = (\sum_{jet} E_T e^{-\eta})/2yE_e$.

The measured $d\sigma/dx_\gamma$ distributions, compared to NLO calculations, are shown in Fig. 4 for ZEUS (left) in four E_T^{jet} ranges, and for H1 (right) in two E_T^{jet} ranges. The relative differences between data and calculations are shown in Fig. 5 for ZEUS (left) and H1 (right). For ZEUS, the agreement between data and calculations in the highest

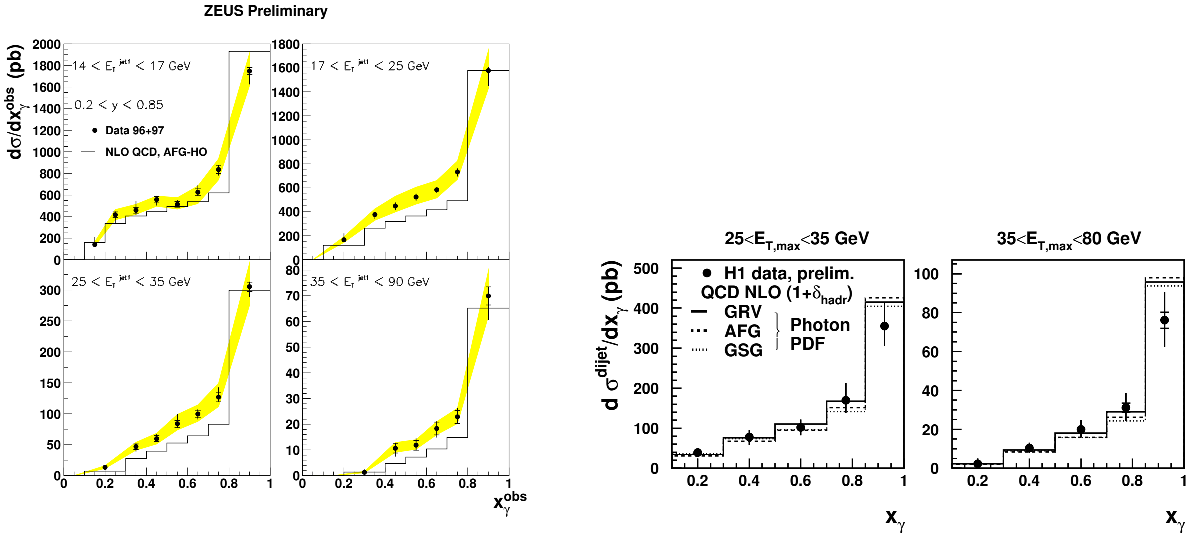

Figure 4. $d\sigma/dx_{\gamma,jets}$ for dijet events, measured by ZEUS (left) for four E_T^{jet} ranges, and by H1 (right) for two E_T^{jet} ranges.

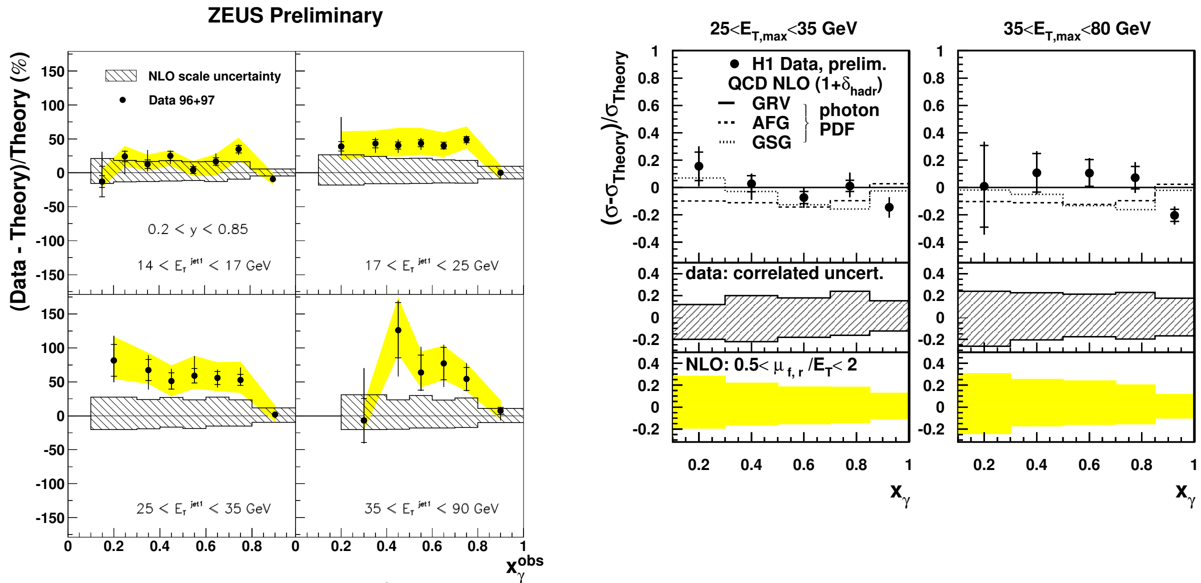

Figure 5. $d\sigma/dx_{\gamma,jets}$: relative differences between data and NLO calculations of the same measurements as in Fig. 4 for ZEUS (left) and H1 (right).

x_γ bin for all E_T^{jet} ranges shows that the direct component is well understood. In the intermediate region $0.3 < x_\gamma < 0.8$, there is some disagreement between data and calculations, which increases with E_T^{jet}. When taking into account the uncertainty of the NLO calculations associated with the choice of the renormalization and factorization scales, shown in Fig. 5 (left), the disagreement between the ZEUS results and the NLO calculations is less pronounced. For H1, contrary to ZEUS, all NLO calculations are in agreement with the data in the whole x_γ range. The ZEUS results may point to an inadequacy of available photon pdfs, and to the need for new global fits including all the most recent data. However, the H1 results do not confirm such a need.

The measured $d\sigma/d|\cos\theta^*|$ for two regions of x_γ is presented in Fig. 6. The left part shows the ZEUS results for $x_\gamma > 0.75$ (top), $x_\gamma < 0.75$ (middle) and the comparison

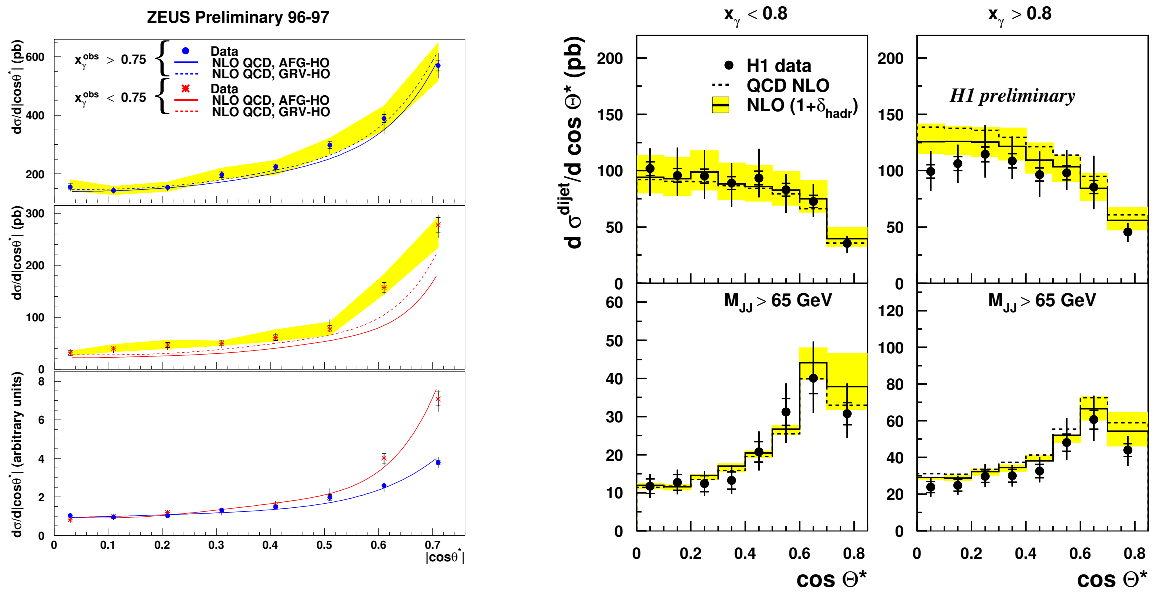

Figure 6. $d\sigma/d|\cos\theta^*|$. Left: ZEUS result for $x_\gamma > 0.75$ (top), $x_\gamma < 0.75$ (middle) and comparison of both shapes (bottom). Right: H1 result for $x_\gamma > 0.8$ (right), and $x_\gamma < 0.8$ (left), without (top) and with (bottom) an additional cut on the jet-jet invariant mass ($M_{jj} > 65$ GeV).

of the shapes of the distributions in both regions (bottom). As discussed in Section 2, the cross-section in the low x_γ region, where resolved processes are dominant, rises faster when $\cos\theta^* \to 1$. The shapes are well described by the calculations, but the normalizations are only well reproduced in the high x_γ region, whereas data are above the calculations in the low x_γ region, which is consistent with the $d\sigma/dx_\gamma$ measurement. The right part shows the H1 results for $x_\gamma > 0.8$ (right), and $x_\gamma < 0.8$ (left). Both normalizations and shapes are well reproduced by the calculations, and the faster rise of the cross-section in the low x_γ region also shows up, as expected, when an additional cut on the jet-jet invariant mass ($M_{jj} > 65$ GeV) is included (bottom) to reduce phase space limitations. Results from both experiments confirm that the spin structure of the partonic interaction is well understood. But, as in the case of the $d\sigma/dx_\gamma$ measurement, a difference persists between ZEUS, which sees a resolved contribution above the calculations, and H1, which is in agreement with the calculations.

However, the NLO calculations were not done in the same way by the two collaborations. ZEUS used the AFG photon pdfs while H1 used GRV, which already gives a 10% higher value, as can be seen in Fig. 5 (right). The value of α_S used, for the matrix elements as well as for the proton pdfs (CTEQ4M for ZEUS and CTEQ5M for H1), gives a 5% larger NLO prediction for H1 compared to that from ZEUS. The hadronization corrections, which were applied to the H1 NLO predictions only, produce a 5% decrease of these predictions compared to the ZEUS ones. All these effects reduce the apparent disagreement between H1 and ZEUS by about 10%, but do not resolve the problem, given that the relative difference between the ZEUS results and the NLO calculations is above 50% in many bins. Further investigation is needed to clarify the situation.

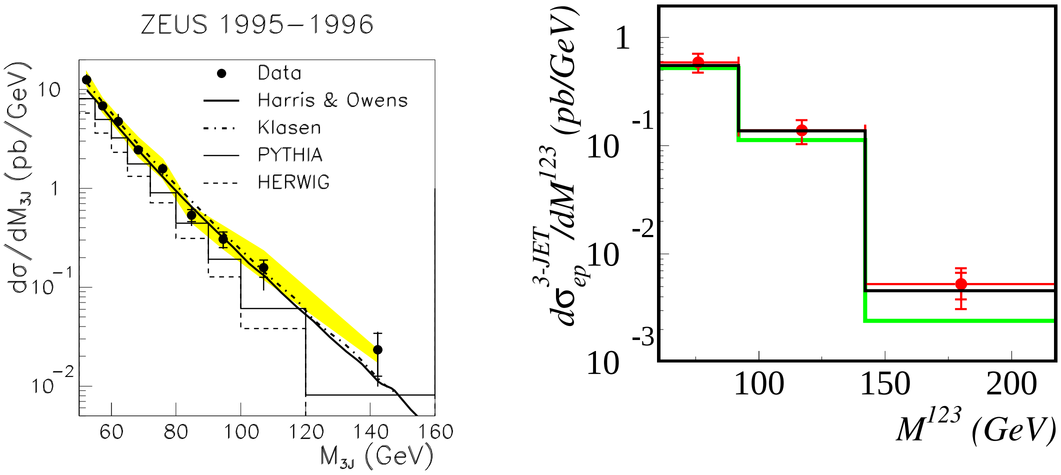

Figure 7. $d\sigma/dM_{jjj}$. Left: ZEUS result compared to $\mathcal{O}(\alpha\alpha_s^2)$ calculations (curves) and to LO Monte-Carlo calculations (histograms). Right: H1 result compared to $\mathcal{O}(\alpha\alpha_s^2)$ calculation of Pötter (dark) and to PYTHIA calculation (grey).

5. 3-jet cross-sections

All QCD tests done with dijet cross-section measurements can be pushed even further using 3-jet measurements. Since a NLO calculation for 3-jet cross-sections in photoproduction is not available, the theoretical calculations suffer from large renormalization and factorization scale uncertainties. The measurements thus represent a challenge for future theoretical work. Up to now, data can be compared to LO Monte-Carlo including parton showers, or to available $\mathcal{O}(\alpha\alpha_s^2)$ calculations [22, 23, 24]. The several possible mass combinations of either 2 of the 3 jets, or the 3-jet invariant mass itself are interesting variables to look for new phenomena. The ability of theoretical calculations to reproduce the rich topology of the event is also a good test of the validity of QCD in a new kinematic domain.

A 3-jet event can be characterized by 5 independent parameters: M_{jjj}, X_3, X_4, $\cos\theta_3$, ψ_3. Using the notation of jets 3, 4, 5 arising from the three outgoing partons in decreasing E_T^{jet}, these variables have the following meaning:

- M_{jjj} is the 3-jet invariant mass;
- $X_i \equiv \frac{2E_i}{M_{jjj}}$ is the energy fraction taken by jet i;
- $\cos\theta_3 \equiv \frac{\vec{p}_B\cdot\vec{p}_3}{|\vec{p}_B||\vec{p}_3|}$ is the polar angle of the leading jet;
- $\cos\psi_3 \equiv \frac{(\vec{p}_3\times\vec{p}_B)\cdot(\vec{p}_4\times\vec{p}_5)}{|\vec{p}_3\times\vec{p}_B||\vec{p}_4\times\vec{p}_5|}$ is the angle between the plane containing the 2 softest jets and the plane defined by the beam axis and the leading jet.

For the 3-jet cross-section measurements published by ZEUS [25], the jets were selected with low E_T^{jet} thresholds: $E_T^{jet} > 6, 6, 5$ GeV, for the 3 most energetic jets of the event, in the η range $|\eta_{jet}| < 2.4$. Further cuts were applied: $M_{jjj} > 50$ GeV, $X_3 < 0.95$, $|\cos\theta_3| < 0.8$. H1 has presented similar preliminary measurements [26], but for higher E_T^{jet} thresholds: $E_{T,jet} > 25, 15, 10$ GeV, for jets in the η range $-0.5 < \eta_{jet} < 2.5$. The 3-jet invariant mass cross-section, is shown in Fig. 7 for ZEUS (left) and H1 (right). The data are well described by $\mathcal{O}(\alpha\alpha_s^2)$ calculations, although with large scale uncertainties,

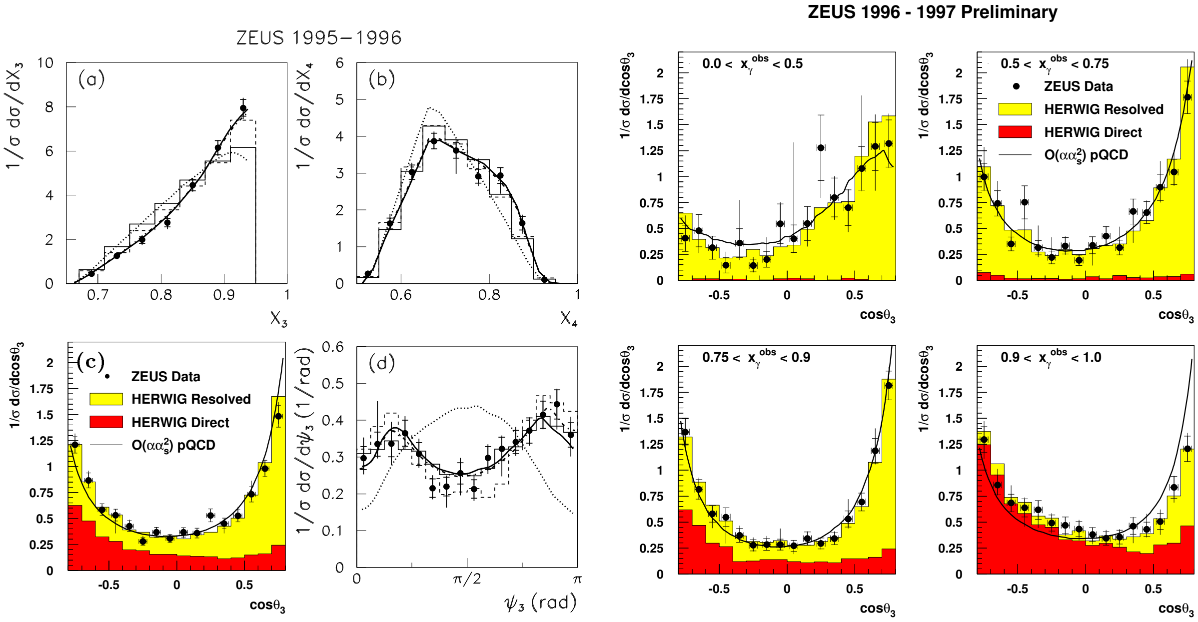

Figure 8. Energy-sharing and angular variables in 3-jet events measured by ZEUS. Left: X_3 (a), X_4 (b), $\cos\theta_3$ (c) and ψ_3 (d). Right: evolution of $\cos\theta_3$ with x_γ.

while the predictions of LO Monte-Carlo simulations are below the data. Unfortunately no resonance in M_{jjj} is seen!

The energy-sharing and angular variables measured by ZEUS are presented in Fig. 8 (left) and compared to PYTHIA, HERWIG, and a pure phase-space model. There is a good general agreement of the QCD calculations with the measurements, whereas the pure phase-space model completely fails to reproduce the ψ_3 distribution. Parton showers with color coherence effects taken into account, as used by HERWIG, give the best description of the data, but the Lund string model used by PYTHIA also adequately describes the data, given the theoretical as well as experimental uncertainties.

The $\cos\theta_3$ distribution presented in Fig. 8(c), which comes from a ZEUS preliminary measurement [27] based on 1996-1997 data, shows that the hardest jet tends to align with the beam axis. This jet is expected, from kinematic arguments, to be preferentially emitted in the proton direction at low x_γ; its chances to be emitted in the photon direction should then increase with x_γ. Indeed, this is what happens, as shown on Fig. 8 (right), where $d\sigma/d\cos\theta_3$ is presented in four x_γ regions. The evolution expected is well reproduced by HERWIG. The $\mathcal{O}(\alpha\alpha_s^2)$ prediction also shows good agreement with data except for the region $0.9 < x_\gamma < 1$.

6. Prompt photons

Prompt photon events provide an interesting tool to test QCD, in a way which is complementary to jets. The direct production of a prompt photon accompanied by a jet involves only the QED Compton diagram ($\gamma + q \rightarrow q + \gamma$) at LO. In the absence of higher-order processes and of an intrinsic transverse momentum (k_T) of the incoming parton inside the proton, the photon and the jet would be balanced in p_T. The observation of

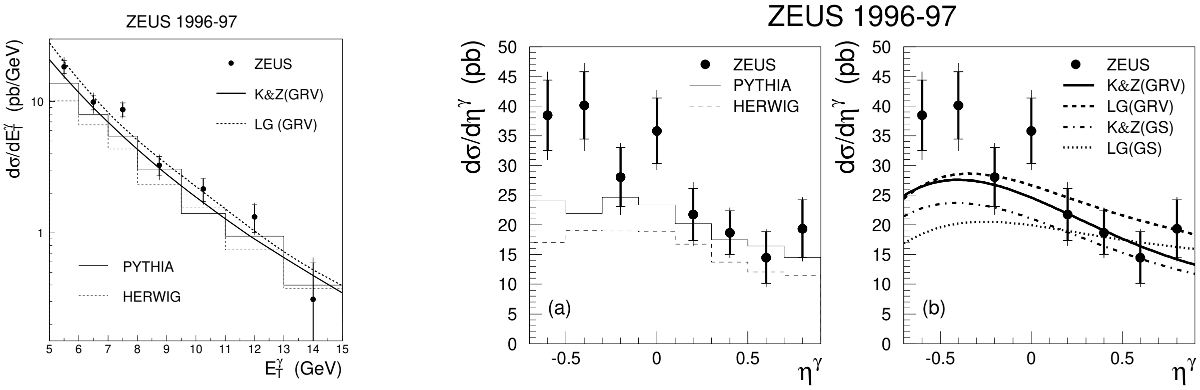

Figure 9. $d\sigma/dE_T^\gamma$ (left) and $d\sigma/d\eta^\gamma$ (center and right) measured by ZEUS in prompt photon events.

p_T imbalance between the photon and the jet thus allows a measurement of the mixed influence of higher-order processes and the intrinsic k_T of partons in the proton.

Isolated photons have been selected by ZEUS [28] with $E_T^\gamma > 5$ GeV in the η range $-0.7 < \eta^\gamma < 0.9$. The dominant uncertainty comes from the modelling of the shower shape of the photon in the calorimeter, which implies a systematic uncertainty of $\pm 8\%$ on the cross-section. The differential cross section $d\sigma/dE_T^\gamma$ is presented in Fig. 9 (left), and compared to PYTHIA and HERWIG LO calculations (histograms) and to NLO QCD calculations (curves) of K&Z [29] and LG [30] using GRV photon pdfs. Both NLO calculations are in good agreement with the data. As in the case of inclusive jet production (see Fig. 3(c)), although less significantly, LO Monte-Carlo calculations, and especially HERWIG, undershoot the measured values, in particular in the low E_T^γ domain. The $d\sigma/d\eta^\gamma$, integrated over $5 < E_T^\gamma < 10$ GeV in the whole y range is also presented in Fig. 9 and compared to LO Monte-Carlo predictions (center) and to NLO QCD calculations using either GRV or GS as photon pdfs (right). These theoretical predictions do not describe the data in the $\eta^\gamma < 0$ region.

To try to pin down the origin of the disagreement, the data were studied separately in 3 different y ranges ($0.2 < y < 0.32$, $0.32 < y < 0.5$, $0.5 < y < 0.9$). It was observed that the disagreement begins to appear for the intermediate y range, and is most prominent for the lowest y range. The inadequacy of the photon pdfs at intermediate x_γ is again suspected, although the measurements are not precise enough to draw any firm conclusion. A more detailed discussion can be found in these proceedings [31].

In a more recent publication [32], ZEUS used the same sample of prompt photons to select direct events ($x_\gamma > 0.9$), where the photon was accompanied by a jet of $E_T^{jet} > 5$ GeV in the η range $-1.5 < \eta_{jet} < 1.8$. Three (non-independent) kinematic variables were used to describe the momentum imbalance of the photon + jet system in the transverse plane: $p_\perp$ (the transverse momentum of the photon with respect to the jet axis), $\Delta\phi$ (the angle between the photon and the jet in the transverse plane), and $p_\parallel$ ($p_\gamma - p_{jet}$ along the jet axis).

The geometric significance of $p_\perp$ and $\Delta\phi$ is presented in Fig. 10(a). The (uncorrected) distributions of these three variables measured by ZEUS are presented in Fig. 10(b,c,d) and compared to a PYTHIA simulation made with three different values

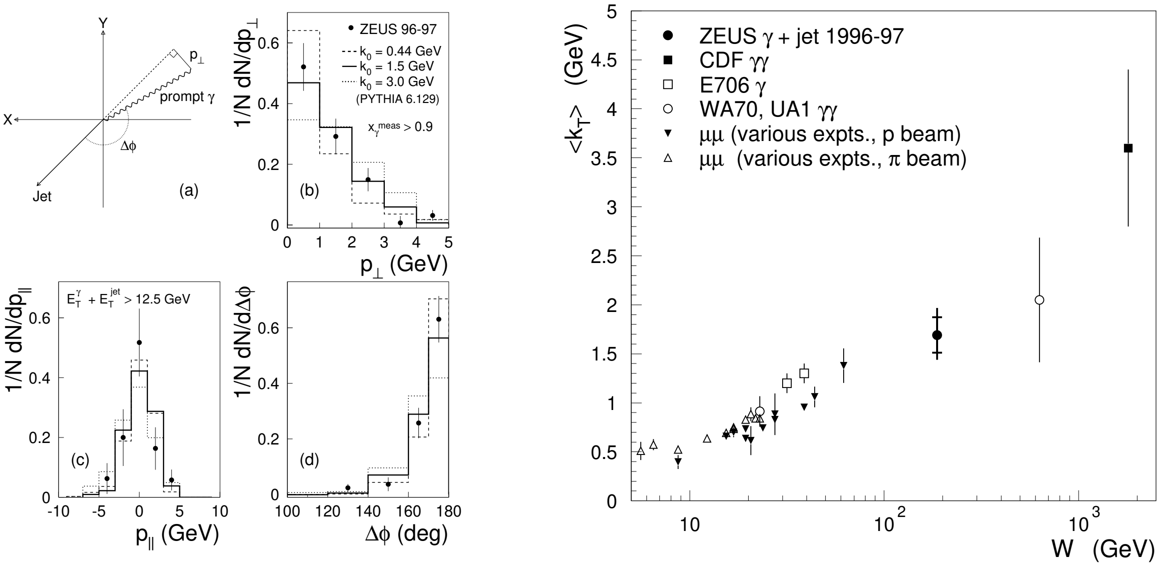

Figure 10. Left: (a) prompt photon + jet transverse momentum imbalance variables. (b) $p_\perp$, (c) $p_{||}$ and (d) $\Delta\phi$ measured by ZEUS. Right: effective $< k_T >$ of partons in the proton, measured by ZEUS, compared to results of several hadron-hadron experiments.

of k_0, where the intrinsic k_T of partons in the proton was assumed to be Gaussian with a width of k_0. Data clearly favour k_0 values in the range 1-2 GeV, and a fitted value of intrinsic $< k_T > = 1.25$ GeV was found, which gave the best agreement between Monte-Carlo simulation and data. Summing quadratically this value of intrinsic k_T with the expected contribution from higher-order processes estimated by PYTHIA gives an effective k_T of $< k_T > = 1.69$ GeV, which can be compared with values obtained by other experiments, as shown in Fig. 10 (right). This result confirms the universality of the rise of the effective $< k_T >$ of the partons inside the proton with the centre-of-mass energy of the hadronic system W.

7. Summary

The results obtained by H1 and ZEUS with the study of jets and prompt photons confirm the consistency of the QCD picture of high E_T photoproduction at HERA. The LO Monte-Carlo simulations reproduce well the detailed characteristics of jets and the topology of dijet or 3-jet events, but their cross-section predictions undershoot the data, for example in inclusive jet or prompt photon production. In the most accurate measurements, data have reached a level of precision high enough as to necessitate the introduction of the NLO contribution to the cross-section calculations. NLO calculations reproduce the data quite well, with some exceptions: ZEUS sees some hints for the need of an improvement of the available photon pdfs, while H1 observes a good agreement between the data and the NLO prediction using the same photon pdfs. Theoretical as well as experimental uncertainties have to be reduced to clarify the situation, and, hopefully, to discriminate between photon pdfs. Using prompt photon events, the effective $< k_T >$ of the partons inside the proton is extracted, and found to be in good agreement with similar measurements at hadron-hadron colliders.

Acknowledgements

I wish to thank B. Kniehl and the organizing commitee for this fruitful meeting, and the conference secretary R. Jurgeleit for her efficient work and friendly welcome. I would also like to thank M. Wing, S. Caron and G. Grindhammer for their help in preparing the presentation, and G. Bernardi, P. Schleper, and J. Whitmore for their comments on the manuscript.

References

[1] M. Klasen, Proc. of the Ringberg Workshop "New Trends in HERA Physics 1999", Ringberg Castle, Tegernsee (Germany), 30 May - 5 June 1999.
[2] R. Wallny, talk at EPS HEP 2001, Budapest (Hungary), 12-18 July 2001;
A. Cooper-Sarkar, talk at EPS HEP 2001, Budapest (Hungary), 12-18 July 2001;
C. Adloff *et al.* [H1 Coll.], *Eur. Phys. J.* C 21 (2001) 33;
J. Breitweg *et al.* [ZEUS Coll.], *Phys. Lett.* B 487 (2000) 53.
[3] R. Nisius, talk at PHOTON 2001, Ascona (Switzerland), 2-7 Sept 2001.
[4] S.D. Ellis and D.E. Soper, *Phys. Rev.* D 48 (1993) 3160.
[5] T. Sjöstrand, *Comput. Phys. Commun.* 82 (1994) 74.
[6] G. Marchesini *et al.*, *Comput. Phys. Commun.* 67 (1992) 465.
[7] B. Andersson *et al.*, *Phys. Rep.* 97 (1983) 31.
[8] B.R. Webber, *Nucl. Phys.* B 238 (1984) 192.
[9] S. Frixione *et al.*, *Nucl. Phys.* B 467 (1996) 399.
[10] M. Klasen and G. Kramer, *Z. Phys.* C 72 (1996) 107.
[11] B.W. Harris and J.F. Owens, *Phys. Rev.* D 57 (1998) 5555.
[12] P. Aurenche *et al.*, Proc. of the Workshop "Future physics at HERA" (1996) 570.
[13] H.L. Lai *et al.*, *Eur. Phys. J.* C 12 (2000) 375.
[14] M.Glück, E. Reya and A. Vogt, *Phys. Rev.* D 46 (1992) 1973.
[15] P. Aurenche *et al.*, *Z. Phys.* C 64 (1994) 621.
[16] L.E. Gordon and J.K. Storrow, *Nucl. Phys.* B 489 (1997) 405.
[17] ZEUS Coll., contributed paper #906 to ICHEP 2000, Osaka (Japan), 27 July - 2 August 2000.
[18] ZEUS Coll., contributed paper #812 to ICHEP 98, Vancouver (Canada), 23-29 July 1998.
[19] H1 Coll., contributed paper #813 to EPS HEP 2001, Budapest (Hungary), 12-18 July 2001.
[20] ZEUS Coll., contributed paper #1066 to ICHEP 2000, Osaka (Japan), 27 July - 2 August 2000.
[21] H1 Coll., contributed paper #798 to EPS HEP 2001, Budapest (Hungary), 12-18 July 2001.
[22] M. Klasen, *Eur. Phys. J.* C 7 (1999) 225.
[23] B.W. Harris and J.F. Owens, *Phys. Rev.* D 56 (1997) 4007.
[24] B. Pötter, *Comput. Phys. Commun.* 119 (1999) 45.
[25] J. Breitweg *et al.* [ZEUS Coll.], *Phys. Lett.* B 443 (1998) 394.
[26] H1 Coll., contributed paper #977 to ICHEP 2000, Osaka (Japan), 27 July - 2 August 2000.
[27] ZEUS Coll., contributed paper #544 to EPS HEP 99, Tampere (Finland) 15-21 July 1999.
[28] J. Breitweg *et al.* [ZEUS Coll.], *Phys. Lett.* B 472 (2000) 175.
[29] M. Krawczyk and A. Zembruski, hep-ph/9810253.
[30] L.E. Gordon, *Phys. Rev.* D 57 (1998) 235.
[31] M. Krawczyk, these proceedings.
[32] S. Chekanov *et al.* [ZEUS Coll.], *Phys. Lett.* B 511 (2001) 19.